Supporting Information for

Tailoring interleaflet lipid transfer with a DNA-based synthetic enzyme

Diana Sobota[a], Himanshu Joshi[b], Alexander Ohmann[a], Aleksei Aksimentiev[b,c], Ulrich F. Keyser[a]

[a]Cavendish Laboratory, University of Cambridge, JJ Thomson Avenue, Cambridge, CB3 0HE, United Kingdom

[b]Department of Physics, University of Illinois at Urbana−Champaign, 1110 West Green Street, Urbana, Illinois 61801, United States

[c]Beckman Institute for Advanced Science and Technology, University of Illinois at Urbana-Champaign, 405 North Mathews Avenue, Urbana, Illinois 61801, United States

Contents

DNA nanostructure assembly

All the reagents used in this work were acquired from Sigma Aldrich, unless stated otherwise. Each single strand was analysed using the NUPACK suite[1], in order to prevent formation of secondary structures, and to ensure sufficient yield of folding. Oligonucleotides modified with an internal C12 spacer were obtained from biomers.net, while unmodified strands and end modifications (TEG (triethylene glycol) -cholesterol anchors, Cy3 labels) were provided by Integrated DNA Technologies, Inc. All the strands were dissolved to a final concentration of 100 μM: unmodified ones in IDTE buffer (10 mM Tris, 0.1 mM EDTA (Ethylenediaminetetraacetic acid), pH 8.0) and the modified in Milli-Q purified water. Strands were then stored at 4 °C, except for dye-modified ones, which were stored at -20 °C.

In order to fold the designed structures, the strands were mixed to a final concentration of 1μM in TE20 buffer (10 mM Tris, 1 mM EDTA, 20 mM Mg^{2+}, pH 8.0), with cholesterol-modified strands heated beforehand at 70 °C for 10 min. For UV-vis measurements and PAGE analysis, the structures were folded in a buffer with magnesium concentration stated for each experiment. DNA duplexes were left for half an hour at room temperature before proceeding with experiments. Folded structures were all stored at 4 °C.

Since the 0D has complimentary nucleotides forming a double helix in its central site, while dodecane-modified structures do not, it may be that these additional nucleotides are responsible for the different reaction to magnesium changes; the overall stronger hydrogen bonding between the two strands of 0D DNA may be responsible for its different sensitivity to cation concentration. Therefore, the experiment was performed, comparing not only the three tested structures, but also the additional one (0D()), similar to the 0D structure, but with four unhybridized nucleotides in its central site. This structure forms a similar number of chemical bonds as the 1D and 2D structures, but lacks their chemical modification. For detailed sequences see Supplementary Table 1.

Ionic current measurements

Ionic current measurements were carried out using solvent-containing membranes. Hexadecane (1 % in pentane) was added on both sides of a hole (diameter = 0.1 mm) in the foil dividing *cis* and *trans* chambers of the Teflon cuvette. After 5 minutes of incubation, 700 μL of 0.5 M KCl, 25 mM HEPES (4-(2-hydroxyethyl)-1-piperazineethanesulfonic acid), pH 7.0 was added to each chamber. 5 ml of 5mg/ml DPhPC lipids (1,2-diphytanoyl-sn-glycero-3-phosphocholine, Avanti Polar Lipids) in pentane were added dropwise to each side, then the whole solution was pipette up and down until the membrane was formed. Current data was acquired at a sampling rate of 1 kHz using Axopatch 200B amplifier. After membrane formation, DNA was added to the *cis* side at the final concentration of 10 nM, and the ionic current under 50 mV voltage across the membrane was recorded. Clampex and Clampfit softwares were used to gather and analyze the data. Assuming an ohmic behaviour of the formed pores, conductance was reported as recorded current (I) by voltage (V) (c = I/V). The experiments were repeated three times for each construct, proving the reproducibility of the results. Additional ionic current traces are presented in Supplementary Fig. 16.

All-atom MD simulations

All MD simulations were performed using NAMD2[2]. The all-atom models of the 48 bp-long DNA duplexes having the same sequence used in experiments (Supplementary Table 1) were created using the NAB module of AMBERTOOLs[3]. One cholesterol molecule was covalently conjugated to each strand of dsDNA molecule using a triethylene glycol (TEG) linker, as described previously[4]. The force-field parameters of the cholesterol molecule with the linker were obtained from the CHARMM General Force Field (CGenFF) webserver[5]. The attachment points for the cholesterol molecules on the opposite strands of the duplex were separated by 24 bp, corresponding to approximately 8 nm, see Supplementary Table 1. The dsDNA molecule decorated with two cholesterol attachments (referred to as 0D) was used to build two other systems containing one (1D) or two (2D) dodecane spacers. The spacers were introduced by replacing the four nucleotides with a dodecane molecule, as specified in Supplementary Table 1. Two initial configurations of the 2D structure were constructed, differing by the conformation of the spacers: contracted and stretched (Supplementary Fig. 17). The initial configuration proved to have an effect on the water permeation and lipid flipping, resulting from the differences in pore formation (Supplementary Fig. 18).

Each DNA construct was inserted into a pre-equilibrated patch of 1,2-diphytanoyl-sn-glycero-3-phosphatidylethanolamine (DPhPE) lipid bilayer in a tilted conformation (under a 60° angle to the bilayer normal) to place both cholesterol anchors within the volume occupied by the lipid membrane. All lipid molecules located within 3 Å of the DNA were removed. Mg^{2+}- hexahydrates were added near the backbone of the DNA to neutralize its negative charge, as described previously[6]. The resulting system was solvated with TIP3P water molecules[7] using the Solvate plugin of VMD[8]. Sodium and chloride ions were added to produce a 100 mM solution using the Autoionize plugin of VMD. A few additional Mg^{2+}– hexahydrates and chloride ions were added to result in the 4 mM bulk concentration of $MgCl_2$. Thus assembled systems measured 13 x 23 x 13 nm^3 and contained approximately 346,000 atoms.

The assembled systems were subjected to energy minimization using the conjugate gradient method to remove the steric clashes between the solute and solvent. Following that, we equilibrated the lipid molecules around the DNA for 50 ns, while harmonically restraining all the non-hydrogen atoms of DNA using a spring constant of 1 kcal mol^{-1} $Å^{-2}$. Subsequently, we removed the harmonic restraints and performed 50 ns equilibration while maintaining the hydrogen bonds between the complimentary base-pairs of DNA using the extrabond utility of NAMD. Finally, we removed all the restraints and performed 1 μs long production simulations of systems using a constant number of atoms (N), pressure (P = 1 bar) and temperature (T = 298 K), the NPT ensemble.

All the MD simulation were performed using periodic boundary conditions and particle mesh Ewald (PME) method to calculate the long range electrostatic interactions[9]. The Nose-Hoover Langevin piston[10] and Langevin thermostat were used to maintain the constant pressure and temperature in the system. CHARMM36 force field parameters[11] described the bonded and non-bonded interactions between DNA, lipid bilayer, water and ions. We used the latest NBFIX corrections to improve the non-bonded interaction among DNA and PE lipid headgroups[12]. An 8-10-12 Å cutoff scheme was used to calculate van der Waals and short range electrostatic forces. All simulations were performed using a 2 fs time step to integrate the equation of motion. SETTLE algorithm[13] was applied to keep water molecules rigid, whereas RATTLE algorithm[14] constrained all other covalent bonds involving hydrogen atoms. The coordinates of the system were saved at an interval of 19.2 ps. The analysis and post processing of the simulation trajectories were performed using VMD[8] and CPPTRAJ[3] and an online Fortran program Illustrator was used to visualize the structures[15].

Confocal microscopy imaging

Confocal microscopy images were acquired on an Olympus FluoView filter-based FV1200F-IX83 laser scanning microscope using a 60x oil immersion objective (UPLSAPO60XO/1.35). NBD excitation was performed using a 25 mW 473 nm laser diode at 1 % laser power, with emission collected between 490 and 525 nm. Cy3 excitation was performed using a 1.5 mW 543 nm HeNe laser at 3% laser power, with emission collected between 560 and 590 nm. For time traces of bleaching of NBD images were recorded every 10 s, with a sampling speed of 2.0 µs/pixel. FIJI was used to analyse the images[16]. The chosen imaging parameters (laser power 1 %, 1 frame *per* 10 s) reduced the effects of NBD photobleaching, as presented in Supplementary Figure 22. Following the linear fit to the measured data points, the fluorescence intensity change after 15 min was calculated to be around 2.2 %, more than a factor of 20 lower than any changes due to NBD bleaching by dithionite over the time of the experiments.

Vesicle preparation

Vesicles used in the assay were prepared with electroformation, as reported previously[4]. POPC (1-palmitoyl-2-oleoyl-glycero-3-phosphocholine) and NBD-PC lipids (1-palmitoyl-2-{6-[(7-nitro-2-1,3-benzoxadiazol-4-yl)amino]hexanoyl}-sn-glycero-3-phosphocholine), both acquired from Avanti® Polar Lipids, were used in a ratio of 200:1, with the final concentration of 5 mg/ml in chloroform. 600 µl of 1 M sorbitol in 200 mM sucrose was used as a buffer. The osmolality of the buffer was around 1200 mOsm (Supplementary Table 5), with all the dilution buffers used in the experiments adjusted accordingly. Since for cell plasma the osmolality ranges between 275 - 325 mOsm[18], therefore we do not claim a biological osmolality. All the buffers were adjusted to pH 7.5 (using sodium hydroxide and hydrochloride solutions) - the value within the acidity range observed in natural systems[19].

Dithionite reduction of NBD-lipids

The NBD reduction assay was performed with the same imaging setup as described above. 20 µl of electroformed liposomes were incubated for 2 h with 50 µl of DNA structures diluted in an osmotically balanced glucose-based buffer (Supplementary Table 5). The difference in the sugars' densities caused sucrose-filled vesicles to sediment to the bottom of the incubation chamber. The concentration of DNA in this mixture was 0.11 µM. Immediately preceding the assay, sodium dithionite was diluted in 1 M Tris at pH 10 to a concentration of 15 mM. This solution was further diluted in osmotically balanced glucose solution, from which 30 µl was added to the chamber. The final concentrations of DNA and dithionite were 0.08 µM and 4.5 mM respectively (unless stated otherwise, see below). Vesicles were imaged for 30 min after dithionite addition.

The dithionite-related limitations (especially its degradation in aqueous solutions *via* hydrolysis[20]) prevented us from seeing clear differences between 0D and 1D structures' rates in the + Mg experiment, even though the much slower 2D structure was clearly differing from the other two designs (Supplementary Fig. 19). In order to obtain more information, an additional experiment was performed, with the concentration of dithionite doubled (final 9 mM), and the control with non-inserting structure presented in Supplementary Fig. 20. Figure 3 shows averaged traces from this assay. Analysing the presented plots, it can be noted that a biexponential model of the decay is more prominent with more C12 modifications incorporated in the design. Especially the slowest 2D structure has clearly two phenomena responsible for the decay (Supplementary Fig. 21).

For fitting all of the obtained traces, a biexponential decay equation (1) was chosen to describe initial fast (dithionite acting on the outer layer of the vesicle) and then slow bleaching (further bleaching of flipped lipids).

$$I = I_0 + I_1 \exp\left(-\frac{t}{\tau_1}\right) + I_2 \exp\left(-\frac{t}{\tau_2}\right) \quad (1)$$

I_0 – final intensity (plateau value)
I_1, I_2 – coefficients describing the respective decays in signal
τ_1, τ_2 – characteristic time constants

Time constants were used to derive decay rate λ for each exponent, using (2).

$$\lambda = \frac{1}{\tau} \quad (2)$$

Assessment of DNA constructs' temperature stability using UV-Vis absorption spectroscopy

The effect of magnesium concentration on the stability of 0C DNA constructs was assessed using a UV-Vis spectrophotometer (Cary 300 Bio, Agilent); thermal studies were performed in order to obtain melting curves of the structures. 100 µl of 1 µM DNA sample folded in either 4 mM or 1 mM $MgCl_2$ were heated from 10 to 90 °C, with a heating rate of 1 °C/min. Absorption spectra were collected at 260 nm, and the melting temperature was obtained from the mean of the two linear regions (upper and lower). Representative melting curves are shown in Supplementary Fig. 13. The experiment was repeated three times, and the averaged melting temperature values are plotted in Supplementary Fig. 14, as well as stated in the Supplementary Table 3. The data and its analysis was processed using Origin software for all measurements taken.

Native polyacrylamide gel electrophoresis (PAGE)

Polyacrylamide gel electrophoresis was used to confirm the proper folding of DNA designs. The gels were prepared at a concentration of 10 % polyacrylamide, 0.5x TBE (Tris, borate, EDTA) and with 11 mM $MgCl_2$, unless stated otherwise. Addition of 0.01 vol% ammonium persulfate (APS) (10 %) and 6.7 × 10^{-4} % N,N,N',N' Tetramethylethylenediamine (TEMED) were used to initialise polymerisation, which proceeded for an hour. 2 µl of a DNA sample was mixed with 0.4 µl of 6x loading dye (15 % Ficoll 400, 0.9 % Orange G diluted in Mili-Q water), and then 2 µl of sample were loaded into the well. GeneRuler Low Range ladder (Thermo Fisher Scientific Inc.) was used as a reference. The gel was run in a Mini-PROTEAN Tetra Cell (Bio-Rad), in 0.5x TBE with 11 mM $MgCl_2$ (unless stated otherwise) at 100 mV for 90 min. After this time the gel was immersed for 10 min in GelRed (Biotium), in order to stain the DNA. The imaging was performed on a GelDoc-It TM (UVP). FIJI was used to analyse gel images.

References

1. Zadeh, J. N. *et al.* NUPACK: Analysis and design of nucleic acid systems. *J. Comput. Chem.* 2011, 32(1) doi:10.1002/jcc.21596.
2. Phillips, J. C. *et al.* Scalable molecular dynamics with NAMD. *J. Comput. Chem.* 2005, 26(16): 1781-1802, doi:10.1002/jcc.20289.
3. Case, D. A. *et al.* AMBER14. *AMBER 14* (2014).
4. Ohmann, A. *et al.* A synthetic enzyme built from DNA flips 107 lipids per second in biological membranes. *Nat. Commun.* 2018, 9(1) doi:10.1038/s41467-018-04821-5.
5. Vanommeslaeghe, K. & MacKerell, A. D. Automation of the CHARMM general force field (CGenFF) I: Bond perception and atom typing. *J. Chem. Inf. Model.* 2012, 52(12): 3144-3154, doi:10.1021/ci300363c.
6. Göpfrich, K. *et al.* Large-Conductance Transmembrane Porin Made from DNA Origami. *ACS Nano* 2016, 10(9): 8207-8214, doi:10.1021/acsnano.6b03759.
7. Jorgensen, W. L., Chandrasekhar, J., Madura, J. D., Impey, R. W. & Klein, M. L. Comparison of simple potential functions for simulating liquid water. *J. Chem. Phys.* 1983, 79: 926-935, doi:10.1063/1.445869.
8. Humphrey, W., Dalke, A. & Schulten, K. VMD: Visual molecular dynamics. *J. Mol. Graph.* 1996, 14(1): 33-38, doi:10.1016/0263-7855(96)00018-5.
9. Darden, T., York, D. & Pedersen, L. Particle mesh Ewald: An N·log(N) method for Ewald sums in large systems. J. Chem. Phys. 1993, 98(12), doi:10.1063/1.464397.
10. Feller, S. E., Zhang, Y., Pastor, R. W. & Brooks, B. R. Constant pressure molecular dynamics simulation: The Langevin piston method. *J. Chem. Phys.* 1995, 103(11), doi:10.1063/1.470648.
11. Hart, K. *et al.* Optimization of the CHARMM additive force field for DNA: Improved treatment of the BI/BII conformational equilibrium. *J. Chem. Theory Comput.* 2012, 8(1): 348-362, doi:10.1021/ct200723y.
12. Yoo, J. & Aksimentiev, A. New tricks for old dogs: Improving the accuracy of biomolecular force fields by pair-specific corrections to non-bonded interactions. *Phys. Chem. Chem. Phys.* 2018, 20(13): 8432-8449, doi:10.1039/c7cp08185e.
13. Miyamoto, S. & Kollman, P. A. Settle: An analytical version of the SHAKE and RATTLE algorithm for rigid water models. *J. Comput. Chem.* 1992, 13(8), doi:10.1002/jcc.540130805.
14. Andersen, H. C. Rattle: A 'velocity' version of the shake algorithm for molecular dynamics calculations. *J. Comput. Phys.* 1983, 52(1): 24-34, doi:10.1016/0021-9991(83)90014-1.
15. Goodsell, D. S., Autin, L. & Olson, A. J. Illustrate: Software for Biomolecular Illustration. *Structure* 2019, 27(11): 1716-1720, doi:10.1016/j.str.2019.08.011.
16. Schindelin, J. *et al.* Fiji: An open-source platform for biological-image analysis. *Nature Methods* 2012, 9(7): 676-682, doi:10.1038/nmeth.2019.
17. Jiang, T., Yu, K., Hartzell, H. C. & Tajkhorshid, E. Lipids and ions traverse the membrane by the same physical pathway in the nhTMEM16 scramblase. *Elife* 2017, 6, doi:10.7554/eLife.28671.
18. Gagné, F. *Biochemical Ecotoxicology: Principles and Methods*. *Biochemical Ecotoxicology: Principles and Methods* (Elsevier: 2014). doi:10.1016/C2012-0-07586-2.
19. Harvey, L. *et al. Molecular Cell Biology. 4th edition*. *Journal of the American Society for Mass Spectrometry* (New York: W. H. Freeman, 2000). doi:10.1016/j.jasms.2009.08.001.
20. Lister, M. W. & Garvie, R. C. Sodium Dithionite, Decomposition In Aqueous Solution And In The Solid State. *Can. J. Chem.* 1959, 37(9): 1567-1574, doi:10.1139/v59-228.

Supplementary Figures

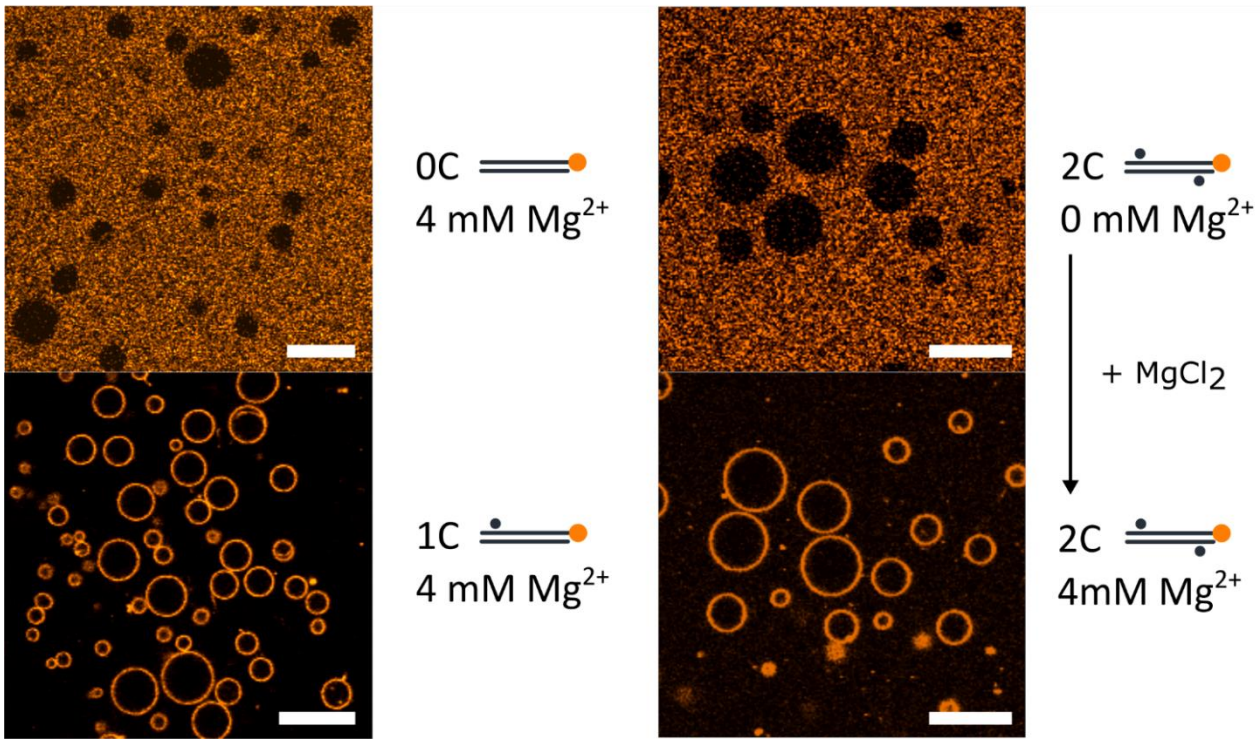

Supplementary Figure 1 Representative microscopy images illustrating membrane attachment of DNA constructs. The signal was collected after exciting Cy3 labels (orange) on DNA. When no anchors are present, no attachment occurs (0C), while even one cholesterol molecule is enough to ensure attachment in the right conditions (1C). When no salt is present in the buffer, no attachment takes place, even with structures with two hydrophobic anchors (2C, 0 mM Mg^{2+}). However, the attachment can be achieved by introducing salt to the same sample (2C, 4 mM Mg^{2+}). Scale bars represent 20 µm.

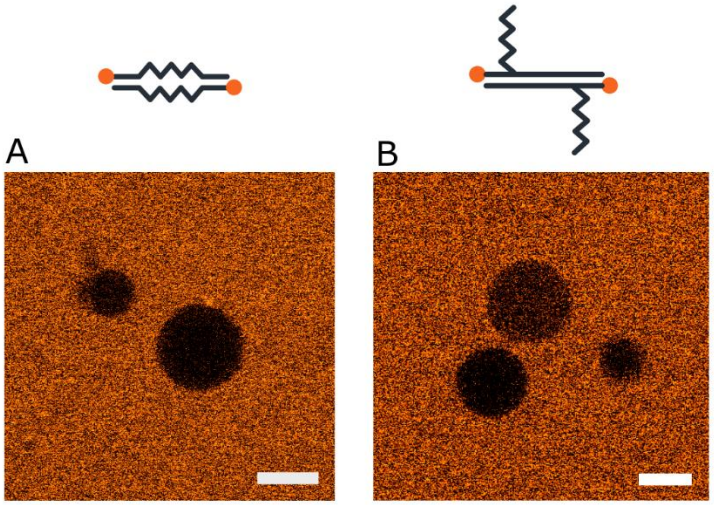

Supplementary Figure 2 Representative microscopy images showing lack of attachment in the absence of cholesterol modifications. Dodecane molecules are not lipophilic enough to ensure DNA anchoring in the membrane, whether they are positioned alongside the DNA duplex (A) or overhang (B). The structures were labelled with Cy3 (orange). The scale bars indicate 5 µm.

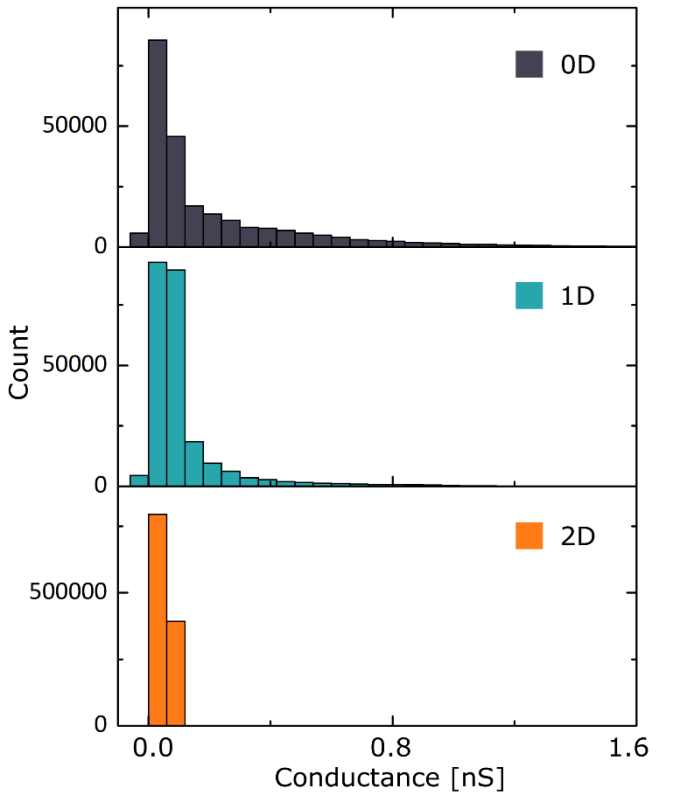

Supplementary Figure 3 All-point histograms of the first 20 minutes of current recordings for three studied designs. In each case the majority of points represent the unaffected bilayer (peak around 0 nS). However, the "tails" of histograms indicate that with increasing hydrophobicity of the central site the higher conductance states appear less frequently.

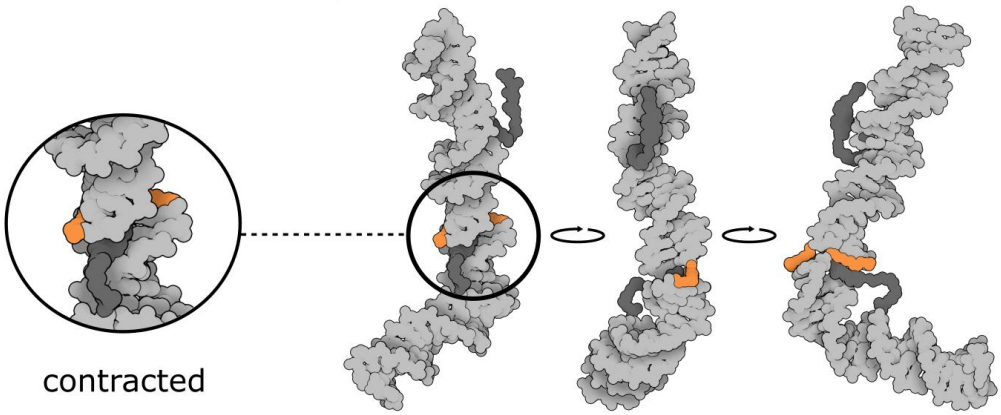

Supplementary Figure 4 Final frame from the simulations of the 2D structure in aqueous solution. Rather than fully stretched, C12 chain adapts a contracted conformation, minimalizing its contact with water.

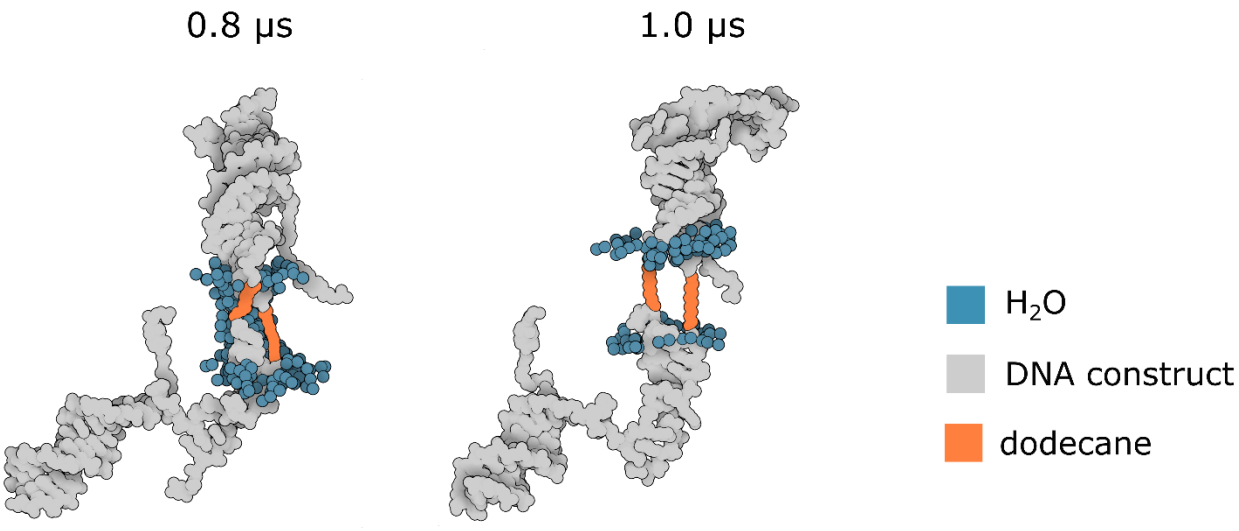

Supplementary Figure 5 Snapshots from the simulations of the 2D structure in a lipid bilayer (omitted for clarity), initially in the folded conformation. After 0.8 μs water molecules are present in the channel, while 200 ns later dodecane chains span through the whole hydrophobic core, pushing DNA, and subsequently water, outside.

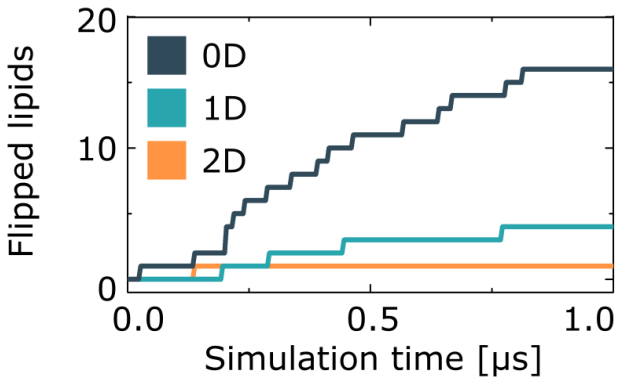

Supplementary Figure 6 Results of all-atom MD simulations, showing lipids transferred between leaflets plotted against time. The 2D structure was simulated in a fully stretched configuration, in order to study the equilibrated system.

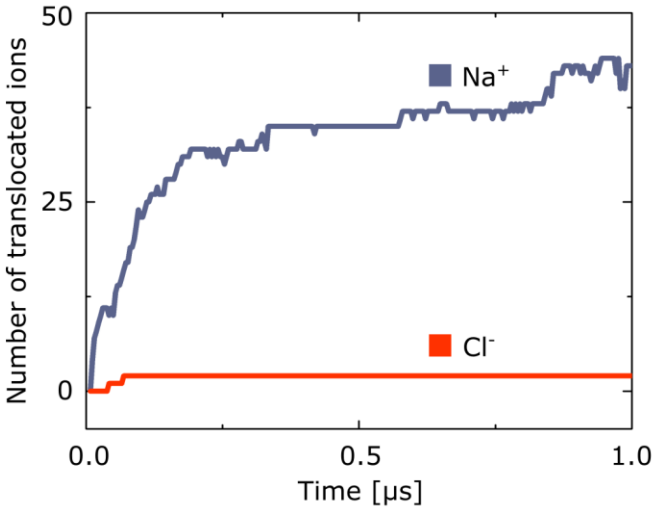

Supplementary Figure 7 Results of all-atom MD simulations, showing the number of ions translocating through the DNA-induced pore (0D).

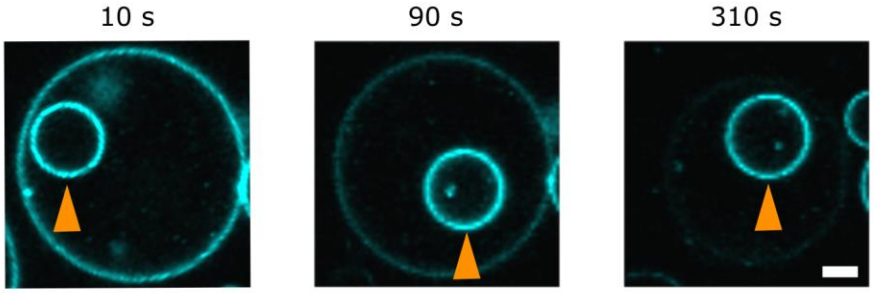

Supplementary Figure 8 Representative micrographs showing a vesicle incubated with 0D structures bleaching after addition of dithionite. The fluorescence of the internal vesicle (orange marker) is not affected throughout the experiment. Scale bar represents 5 µm.

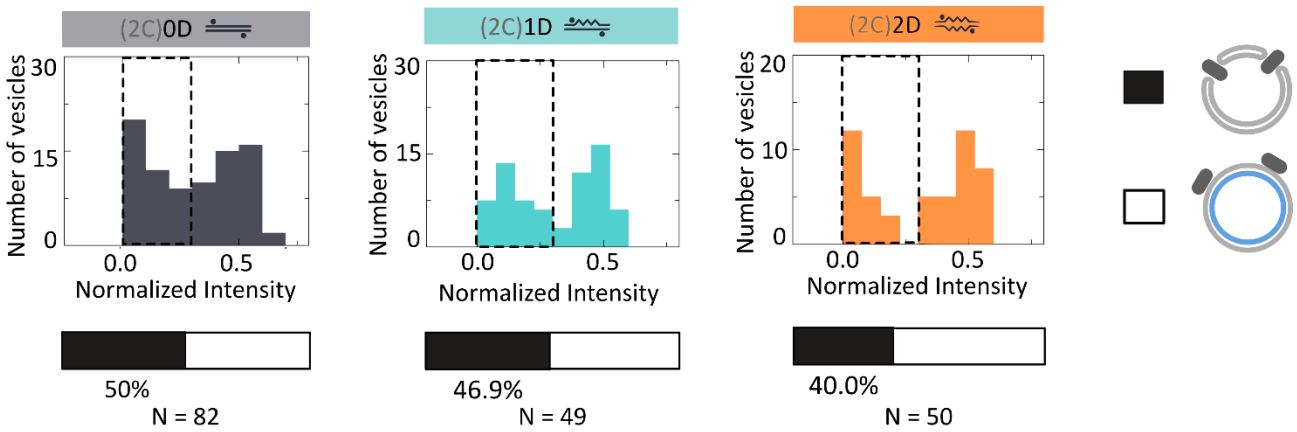

Supplementary Figure 9 Further analysis of the histograms from Fig. 3d (+Mg). By taking into consideration the given amount of traced vesicles, one can roughly estimate the insertion efficiency of studied DNA constructs. For all samples, around half of the vesicles (each ~100 µm^2 membrane area) had no structure inserted – or the insertion was not stable enough to cause noticeable lipid flipping. The decreasing insertion efficiency of C12-modified structures could be explained by their lower stability, however for this sample size the difference cannot be treated as meaningful.

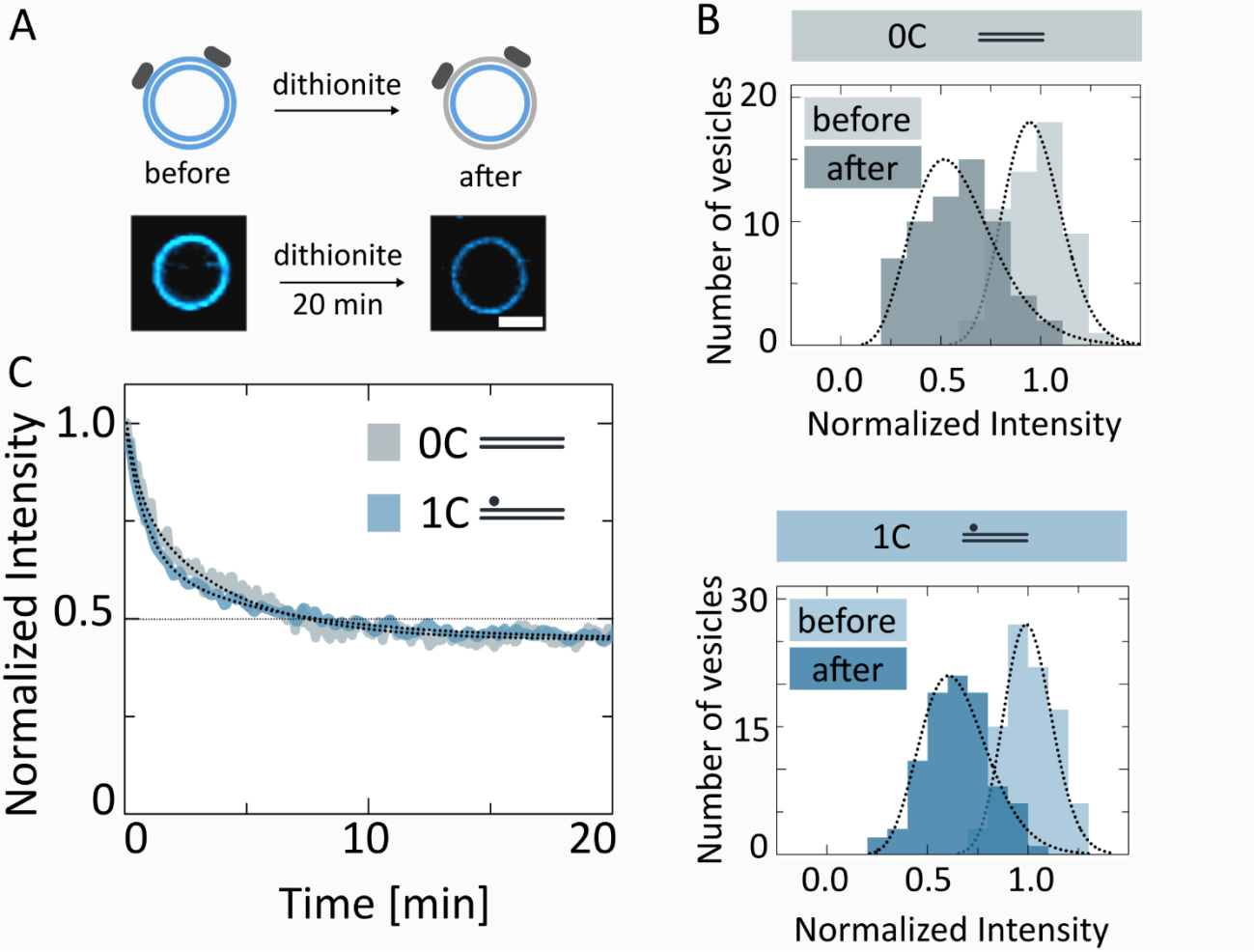

Supplementary Figure 10 Control experiments with non-inserting structures. (A) Illustration of NBD reduction by dithionite: in the absence of the toroidal pore the fluorescence of the inner leaflet stays intact. Representative confocal microscopy images, with scale bar indicating 5 μm. (B) Histograms of the initial and final intensity distribution across the sample for the 1C (N_{before} = 95, N_{after} = 93) and 0C (N_{before} = 55, N_{after} = 60) structures. The dotted lines show Gaussian distribution curves. (C) Fluorescence intensity time traces of NBD-labelled vesicles after dithionite addition at t = 0, in the presence of 0C and 1C constructs. Since no DNA insertion occurs, only the outer leaflet is affected by dithionite, resulting in a 50 % decrease of the signal. Each trace is an average of five vesicles examined across three independent experiments. Dotted lines represent single exponential fits (see Supplementary Table 2 for details).

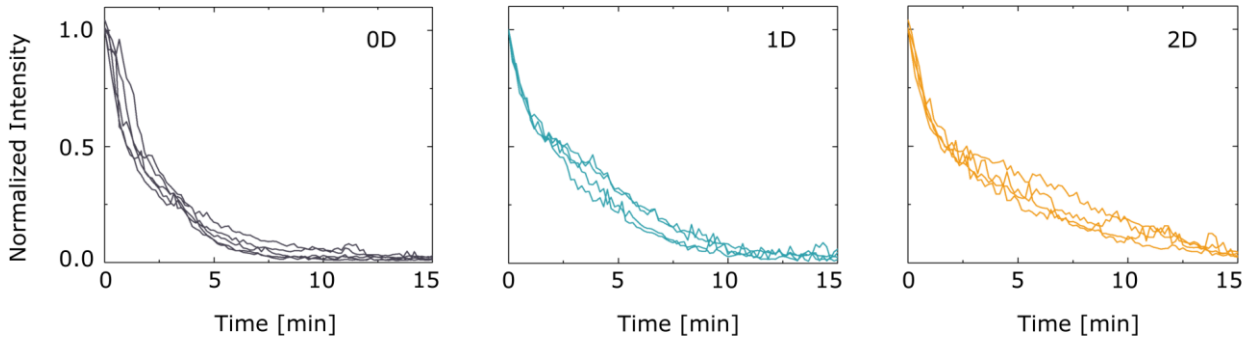

Supplementary Figure 11 Single vesicles' fluorescence decay from the + Mg experiments, with dithionite final concentration = 9 mM.

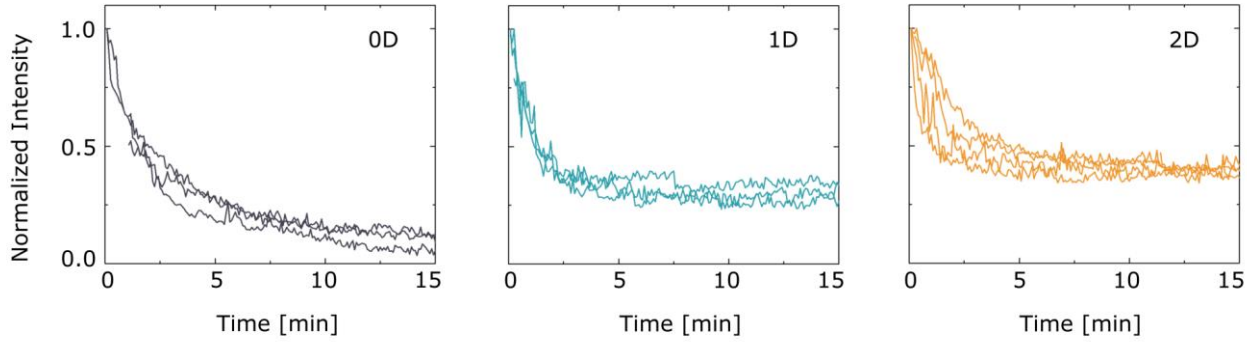

Supplementary Figure 12 Representative traces of fluorescence decay, averaged for the traces from Fig. 3c. The data was collected from at least two separate experiments on three different batches of vesicles.

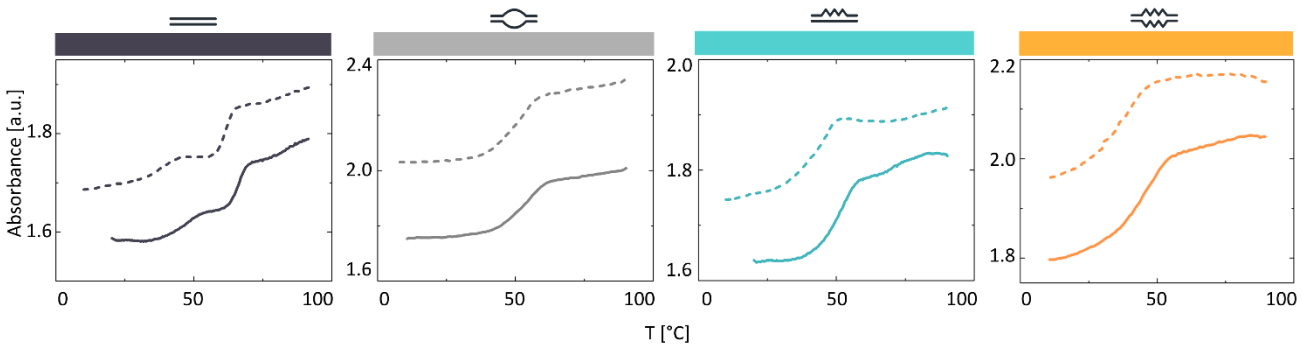

Supplementary Figure 13 Representative melting curves of 0C structures (0D, 1D, 2D, as well as 0D with 4 unhybridized nucleotides in the central site (0D( ), grey)). The data was collected in the presence of 4 mM (continuous line) or 1 mM (dashed line) concentration of magnesium. Looking at the constructs' design (see Fig. 1) one can distinguish two segments of different number of complementary bases: (I) the ends, with 12 nt-long strands designed to carry a cholesterol moiety, and (II) the middle part of 24 bp, with a central site. Since these two segments differ strongly with their length, they will dissociate in different temperatures, which can be observed as two steps on the melting curve of 0D construct (black). However, since for the other three structures we introduced a break (no complementary bases) in the central site, this effect is not visible for them. The melting temperature of the 0D was obtained by treating the curve as a one-step.

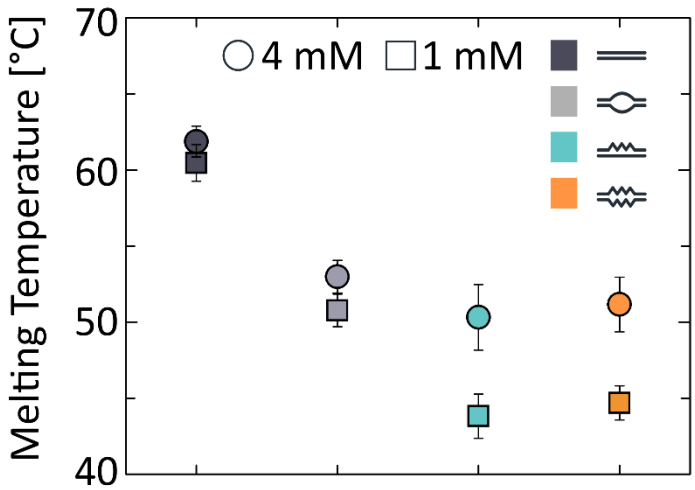

Supplementary Figure 14 Melting temperatures of the studied structures, averaged for three independent experiments. The effect of decreased Mg^{2+} concentration on T_m is especially noticeable for C12-modified designs.

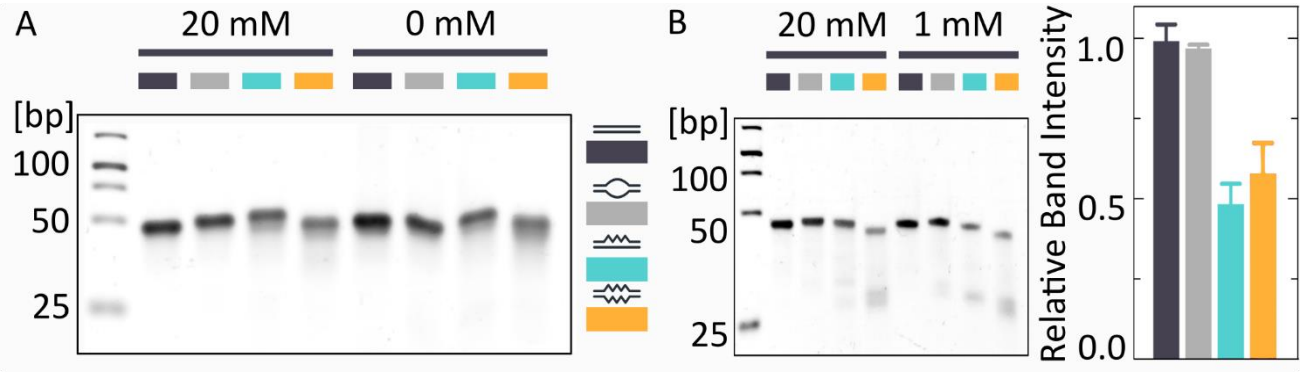

Supplementary Figure 15 PAGE with 11 mM Mg^{2+} (A) or no Mg^{2+} (B). The gels show folding yield for structures in different magnesium concentration. Lower stability of C12-modifed structures can be deduced from the presence of additional, smeared bands below the main band in (B). The bar chart (B) shows 1 mM Mg^{2+} bands' intensity relative to that of the respective 20 mM Mg^{2+} bands. While no change is observed for unmodified structures, the 1D and 2D constructs show around 50% decrease of intensity when in low salt conditions. The error bars represent differences between two experiments. For detailed values see Supplementary Table 4.

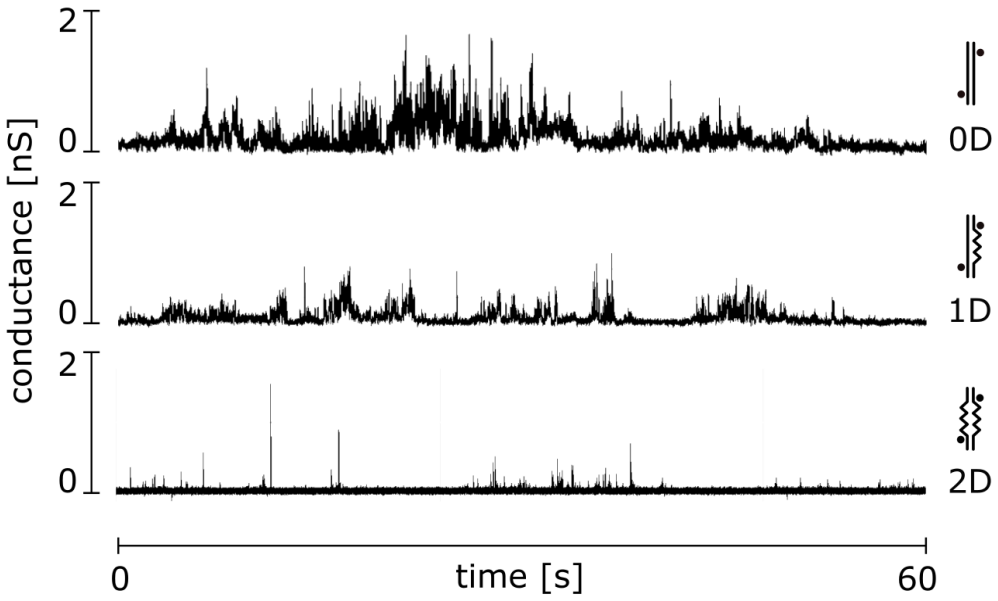

Supplementary Figure 16 Additional examples of conductance traces for each of the measured DNA structures.

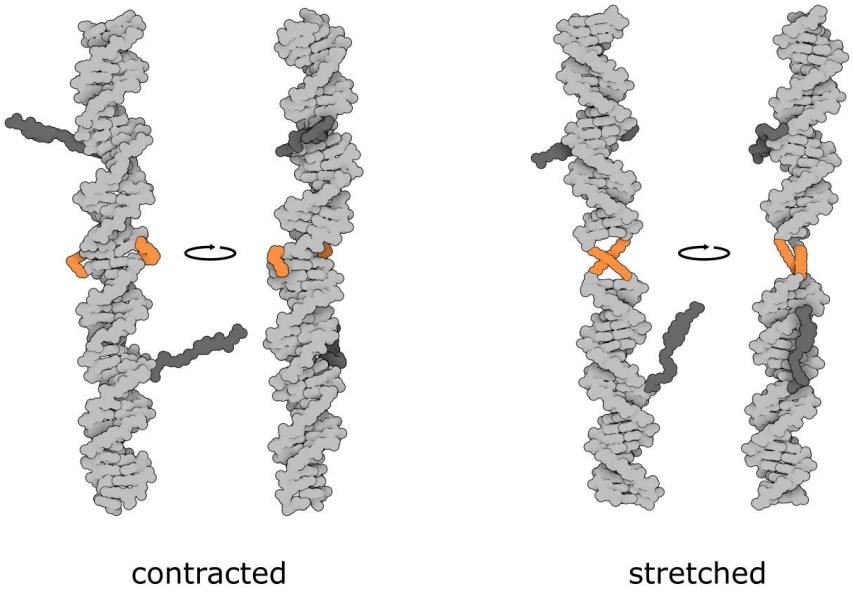

Supplementary Figure 17 Snapshots from the simulations of the 2D structure in its initial configuration either (a) contracted or (b) stretched.

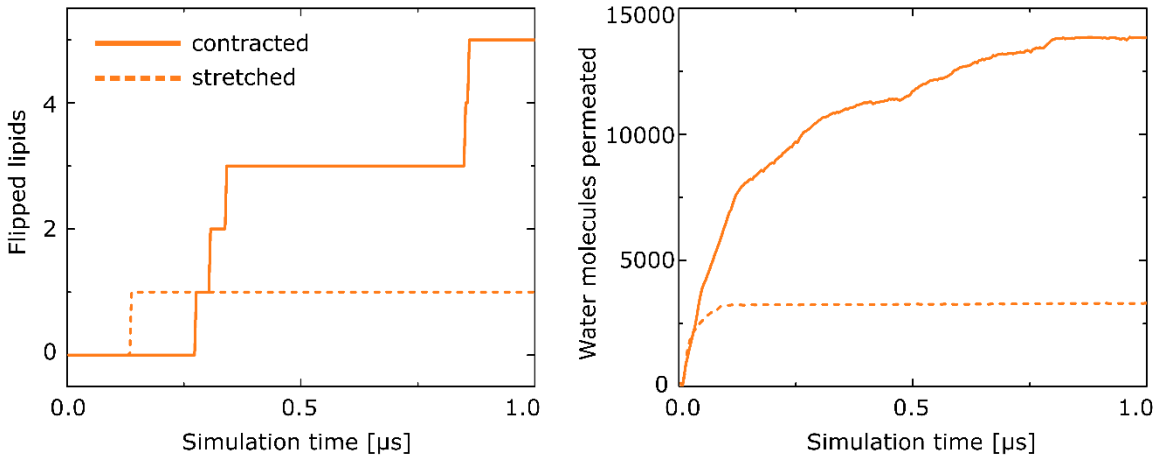

Supplementary Figure 18 Comparison between 2D structure simulated in the membrane in two different initial conformations: contracted and stretched. Contracted conformation of C12 chains is preferred in the solution, while they extend in the hydrophobic core of a bilayer.

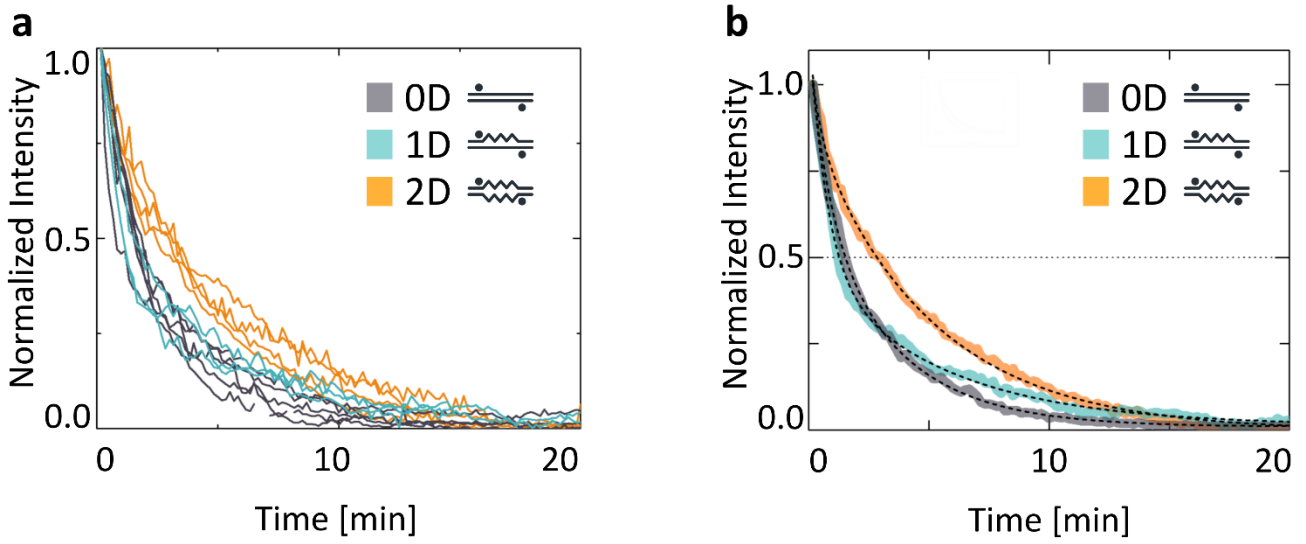

Supplementary Figure 19 Representative traces (a) and their average (b) from the + Mg experiments, with dithionite concentration = 4.5 mM. The data was collected from at least two separate experiments on three different batches of vesicles.

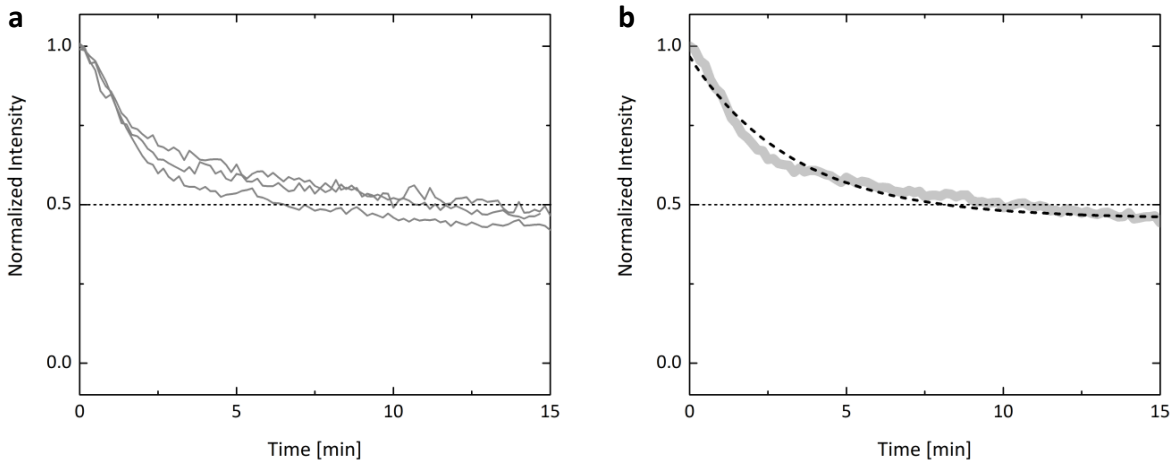

Supplementary Figure 20 Representative traces from the control experiments with non-inserting 1C structures (a), alongside the averaged trace with a dashed line representing single exponential fit (b).

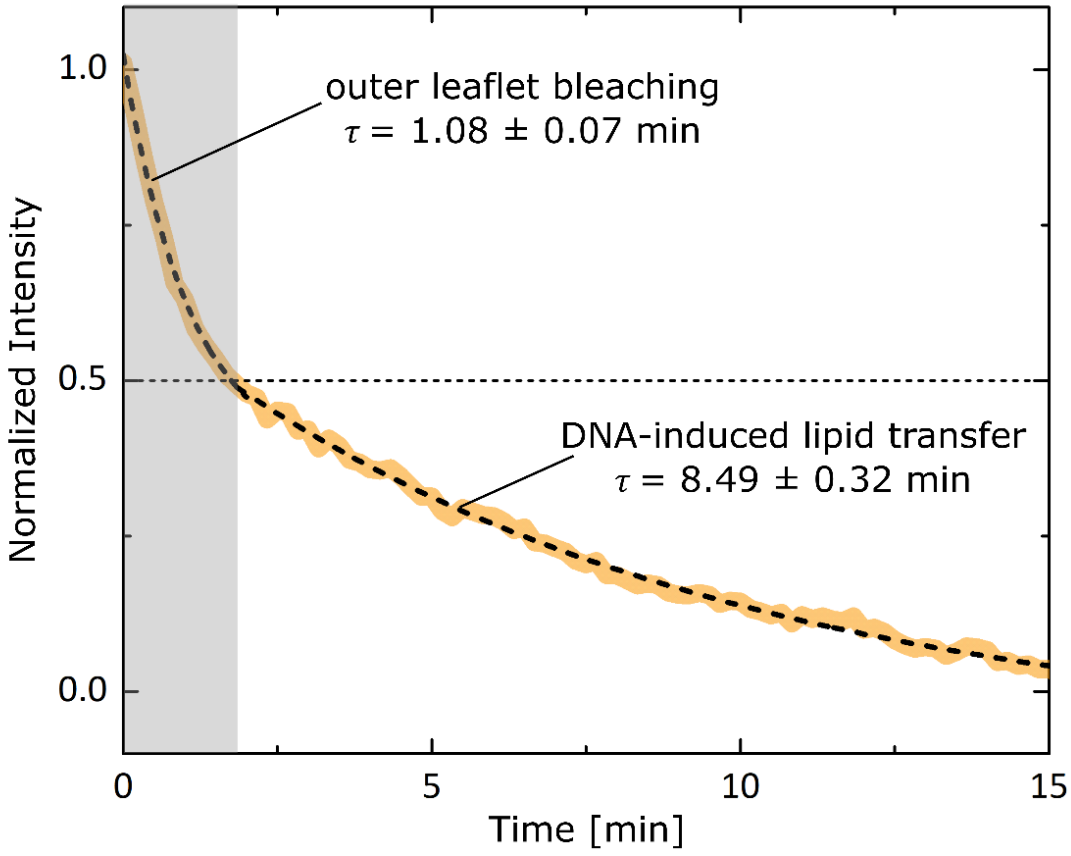

Supplementary Figure 21 The trace from Fig. 3a (2D), fitted with two separate single-exponential functions: either initial 50% fluorescence loss or a subsequent lipid-flipping-induced decay. The two parts of a decay trace, fitted with two separate single exponents representing dithionite bleaching the outer leaflet of a vesicle (grey part), and slower loss of fluorescence caused by the lipid flipping by the DNA-induced pore (white part).

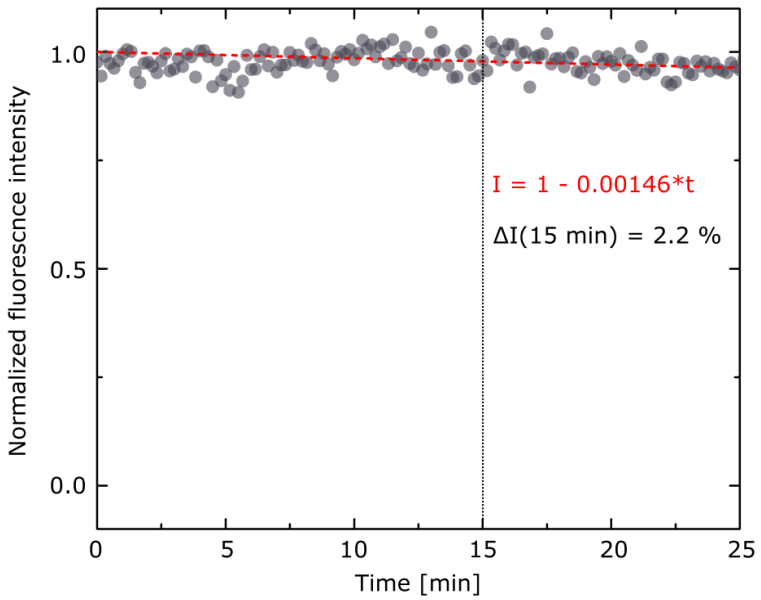

Supplementary Figure 22 The results of a photobleaching experiment, with dashed line representing a linear fit. The dotted line indicates the final frame of the reported NBD reduction assay results. The intensity change due to photobleaching at that point is calculated to be around 2.2 %.

Supplementary Tables

Table 1 Sequences of DNA strands used in this work.

Strand	Sequence (5' > 3')	Length [bp]	Modification
D1	AGTAGTATCCAT	12	3' TEG Cholesterol
D1-0	CATCGTAGCT**AAAA**AAGTCATACATAGATTAGAGAG	36	5' Cy3
D1-S	CATCGTAGCT**(C12)**AAGTCATACATAGATTAGAGAG	32	internal C12
D2	CTCTCTAATCTA	12	3' TEG Cholesterol
D2()-0	TGTATGACTT**AAAA**AGCTACGATGATGGATACTACT	36	
D2-0	TGTATGACTT**TTTT**AGCTACGATGATGGATACTACT	36	
D2-S	TGTATGACTT**(C12)**AGCTACGATGATGGATACTACT	32	internal C12

Table 2 Parameters obtained by fitting double exponential equation to averaged traces of NBD bleaching.

[Mg^{2+}] constant?	[$Na_2S_2O_4$] [mM]	DNA construct	I_0	τ_1 [min]	λ_1 [min^{-1}]	τ_2 [min]	λ_2 [min^{-1}]
+	4.5	0C	0.450 ± 0.001	3.01 ± 0.07	0.33 ± 0.02	-	-
+	4.5	1C	0.458 ± 0.001	3.13 ± 0.06	0.32 ± 0.01	-	-
+	4.5	2C 0D	0.005 ± 0.001	0.94 ± 0.03	1.06 ± 0.03	3.63 ± 0.04	0.28 ± 0.00
+	4.5	2C 1D	0.025 ± 0.004	0.68 ± 0.08	1.47 ± 0.17	4.19 ± 0.19	0.24 ± 0.01
+	4.5	2C 2D	- 0.076 ± 0.008	2.31 ± 0.10	0.43 ± 0.02	9.04 ± 0.30	0.11 ± 0.00
+	9	1C	0.456 ± 0.005	3.31 ± 0.16	0.30 ± 0.01	-	-
+	9	2C 0D	0.012 ± 0.007	1.63 ± 0.29	0.61 ± 0.11	3.89 ± 1.37	0.25 ± 0.01
+	9	2C 1D	-0.014 ± 0.006	0.29 ± 0.06	3.45 ± 0.71	4.66 ± 0.15	0.21 ± 0.01
+	9	2C 2D	-0.164 ± 0.03	0.72 ± 0.05	1.39 ± 0.10	11.66 ± 1.01	0.09 ± 0.01
-	4.5	2C 0D	0.076 ± 0.003	0.91 ± 0.04	1.10 ± 0.05	5.03 ± 0.17	0.20 ± 0.01
-	4.5	2C 1D	0.296 ± 0.003	0.89 ± 0.06	1.12 ± 0.08	3.84 ± 1.39	0.26 ± 0.09
-	4.5	2C 2D	0.388 ± 0.003	1.00 ± 0.06	1.00 ± 0.06	4.92 ± 0.84	0.20 ± 0.03

Table 3 Melting temperatures of DNA constructs.

Construct	T_m [ºC] (4 mM Mg^{2+})	T_m [ºC] (1 mM Mg^{2+})	ΔT_m [ºC]
0D	60.47 ± 1.20	61.87 ± 1.01	1.40 ± 1.57
0D( )	52.99 ± 1.07	50.78 ± 1.07	2.21 ± 1.51
1D	50.31 ± 2.15	43.82 ± 1.45	6.49 ± 2.59
2D	51.16 ± 1.79	44.69 ± 1.12	6.47 ± 2.11

Table 4 Relative band intensities of structures folded in 1 mM Mg^{2+}, normalized to the respective 20 mM Mg^{2+} band, obtained from two independent experiments.

Construct	Normalized intensity (I)	ΔI
0D	0.991	0.053
0D( )	0.968	0.012
1D	0.483	0.064
2D	0.578	0.096

Table 5 Composition and osmolality of buffers used in this work.

Buffer	Sucrose [mM]	Glucose [M]	HEPES [mM]	Sorbitol [M]	Magnesium [mM]	Osmolality [mOsm]
GUVs (inner)	200	-	-	1	-	1200
DNA dilution	-	~1.2 (osmotically balanced)	20	-	4 or 0	1400
Dithionite dilution	-	~1.2 (osmotically balanced)	20	-	4 or 0	1110